Electronic Supplementary Material (ESI) for Nanoscale.
This journal is © The Royal Society of Chemistry 2019

In-place bonded semiconductor membranes as compliant substrates for III-V compound devices

A. J. Garcia Jr.[1], L. N. Rodrigues[1,2], S.Filipe Covre da Silva[1,2,+], S. L. Morelhao[3], O. D. D. Couto Jr.[4], F. Iikawa[4], and Ch. Deneke[1,4,]*

[1]*Laboratório Nacional de Nanotecnologia (LNNano), Centro Nacional de Pesquisa em Energia e Materiais (CNPEM), Campinas, São Paulo, Brasil.*

[2]*Departamento de Física, Universidade Federal de Viçosa (UFV), Viçosa, MG, Brasil*

[3]*Instituto de Física, Universidade de São Paulo (USP), São Paulo, SP, Brasil*

[4] *Instituto de Física "Gleb Wataghin", Universidade Estadual de Campinas (Unicamp), Campinas, SP, Brasil*

[+]*Current address: Johann Kepler Universität, Linz, Austria*

[*]*Corresponding author: cdeneke@ifi.unicamp.br*

Supplemental material

In the supplemental material, we would like to provide some additional information towards samples and sample characterization.

Additional atomic force microscopy images

To complement the surface analysis, Suppl. Fig. 1 and Suppl. Fig. 2 depict AFM images of samples, which have not been added to the discussion of Fig. 2 and Fig. 3 in the main text.

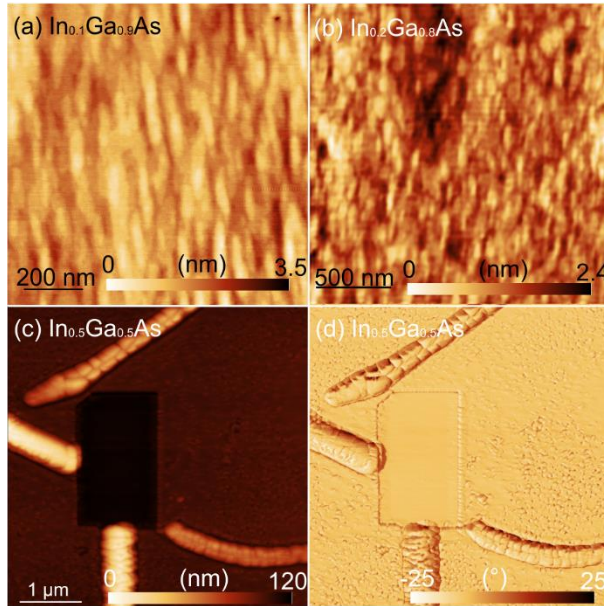

Supp. Figure 1: (a)-(b) Detailed AFM images of a nominally lattice matched (a) 10 nm $In_{0.10}Ga_{0.90}As$ and (b) the 10 nm $In_{0.20}Ga_{0.80}As$ layer on the relaxed membrane. We observe a flat good crystal growth on top of the membrane as well as next to the membrane border. (c)-(d) 10 nm $In_{0.5}Ga_{0.5}As$ film on top of the membrane. We observe material accumulation on top of the wrinkles and some roughing of the surface on the membrane in the topography AFM image (c). Interestingly, the AFM phase image (d) demonstrates that the bare GaAs surface surrounded by the membrane stays essentially flat and without material.

The AFM topography images shown in Suppl. Fig. 1(a) and 1(b) demonstrate that the surface of low Indium content alloys stay flat and exhibit a good layer by layer growth mode. For the 10 nm $In_{0.10}Ga_{0.90}As$ and the 10 nm $In_{0.20}Ga_{0.80}As$ layer we only observe 2D islands on top of the sample and no significant roughing indicating island formation or break down of the epitaxial growth.

As pointed out in the main text, the high Indium content alloys deposited on membrane samples tend to migrate to the top of the membrane and the wrinkles. This is demonstrated by the analysis of the AFM images depicted in Suppl. Fig. 1(c) and 1(d). They show a position in the membrane, where a piece of the membrane misses as it sometimes happens during release and cleaning of the samples. A 10 nm $In_{0.5}Ga_{0.5}As$ film was deposited and AFM topography and phase images obtained. We observe an accusation of the material with the formation of large crystals or islands on top of the wrinkled areas. The phase image clearly demonstrates that no material stays on the bare GaAs surface exposed by the hole in the middle of the sample – in this area the surface stays flat and exhibits just 2D islands of a perfect epitaxial growth.

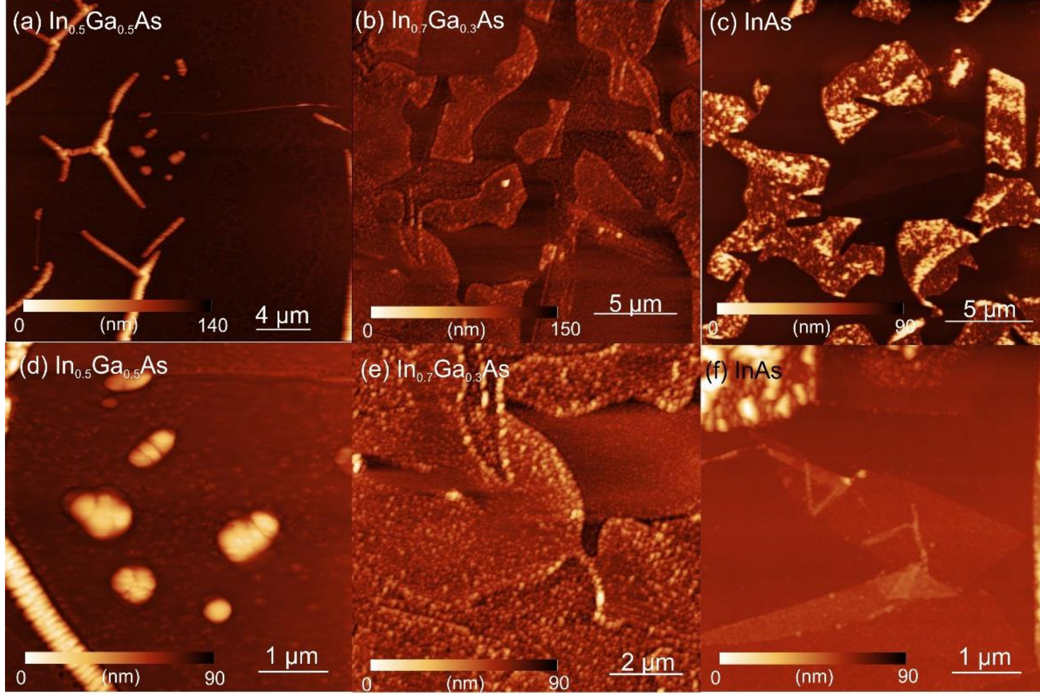

Supp. Fig. 2: Characterization of high Indium content alloys on the membranes. (a) and (d) depict AFM images of a 10 nm $In_{0.5}Ga_{0.5}As$ layer deposited on the membrane of different magnification. We observe the onset off material accumulation on top of the wrinkles and bubble formation between wrinkles. (b) and (e) show overview AFM images of a $In_{0.7}Ga_{0.3}As$ layer. Like for highly strained material – I. e. InAs AFM images in Fig. (c) and (f), we observe huge accumulation and formation of dedicated crystal areas contrary to growth on bare GaAs, where we only obtained a rather homogeneous rough film.

Supp. Fig. 2 depicts AFM images illustrating the complete change of growth for highly strained material on the compliant substrates. Whereas we observe only roughing and island formation for a bare bulk GaAs crystal (see Fig. 3 in main text), highly strained material like $In_{0.5}Ga_{0.5}As$ (Supp. Fig. 2 (a) and (d)), $In_{0.7}Ga_{0.3}As$ (Supp. Fig. 2 (b) and (e)) and pure InAs (Supp. Fig. 2 (c) and (f)) tend not to form flat layers, but start to massively accumulate on preferred areas, e.g. wrinkles and latter form large crystal islands most likely straining the underlying membrane.

Three-dimensional reciprocal space mapping under gracing incident XRD geometry.

In the reference frame of the laboratory where $\hat{\boldsymbol{x}}$ is downstream along the direct X-ray beam, $\hat{\boldsymbol{y}}$ rest on the horizontal plane, and $\hat{\boldsymbol{z}}$ is in the vertical scattering plane, the incident wavevector is simply $\boldsymbol{k} = (2\pi/\lambda)\hat{\boldsymbol{x}}$ while the diffracted wavevector towards the central pixel of the detector area is

$$\boldsymbol{k}'_d = (2\pi/\lambda)[\cos\theta_d\ \cos\phi_d\,\hat{\boldsymbol{x}} + \cos\theta_d\ \sin\phi_d\,\hat{\boldsymbol{y}} + \sin\theta_d\ \hat{\boldsymbol{z}}] = (2\pi/\lambda)\hat{\boldsymbol{s}}_d$$

where θ_d and ϕ_d are the elevation and azimuth angles of the detector arm, respectively.[22] For a detector area perfectly perpendicular to $\hat{\boldsymbol{s}}_d$, and pixel arrays well aligned along vertical and horizontal directions, the position of each pixel can be ascribed as

$$\boldsymbol{r}_d(m,n) = p[(m-m_0)\hat{\boldsymbol{x}}_d + (n-n_0)\hat{\boldsymbol{y}}_d]$$

regarding the position of the central pixel of array indexes m_0 n_0. p = 0.172mm is the pixel size in our case, $\hat{\boldsymbol{x}}_d = -\sin\theta_d\,\cos\phi_d\,\hat{\boldsymbol{x}} - \sin\theta_d\,\sin\phi_d\,\hat{\boldsymbol{y}} + \cos\theta_d\,\hat{\boldsymbol{z}}$, and $\hat{\boldsymbol{y}}_d = -\sin\phi_d\,\hat{\boldsymbol{x}} + \cos\phi_d\,\hat{\boldsymbol{y}}$. In the lab frame, the absolute position of each pixel is therefore given as $\boldsymbol{R} = D\hat{\boldsymbol{s}}_d + \boldsymbol{r}_d(m,n)$ where D is the sample detector distance. The diffracted X-ray intensity at each pixel of indexes m,n has a wavevector $\boldsymbol{k}' = (2\pi/\lambda)\boldsymbol{R}/|\boldsymbol{R}|$, and a reciprocal diffraction vector $\boldsymbol{Q} = \boldsymbol{k}' - \boldsymbol{k}$. The intensity distribution in the sample reciprocal space around a chosen diffraction vector $\boldsymbol{Q}_0$ is obtained after projecting $\boldsymbol{Q}$ in a convenient frame in the reciprocal space of the sample. Here we have used $\hat{\boldsymbol{x}}_s = \cos\theta\,\hat{\boldsymbol{x}} + \sin\theta\,\hat{\boldsymbol{z}}$, $\hat{\boldsymbol{y}}_s = \hat{\boldsymbol{y}}$, and $\hat{\boldsymbol{z}}_s = -\sin\theta\,\hat{\boldsymbol{x}} + \cos\theta\,\hat{\boldsymbol{z}}$ as the sample's reference frame where $\boldsymbol{Q}_0 = Q_0\hat{\boldsymbol{z}}_s$. Therefore, for each step of the incident angle θ, i.e. when rocking the sample around $\hat{\boldsymbol{y}}_s$ in increments of $\Delta\theta$ = 0.01 degrees, the intensity distribution in the vicinity of the diffraction vector $\boldsymbol{Q}_0$ is given as

$$\Delta Q_x = \boldsymbol{Q}\cdot\hat{\boldsymbol{x}}_s,\ \Delta Q_y = \boldsymbol{Q}\cdot\hat{\boldsymbol{y}}_s,\ \text{and}\ \Delta Q_z = \boldsymbol{Q}\cdot\hat{\boldsymbol{z}}_s.$$

In Supp. Fig. 3 there is an example of how the intensity is distributed around the 220 in-plane GaAs reflection.

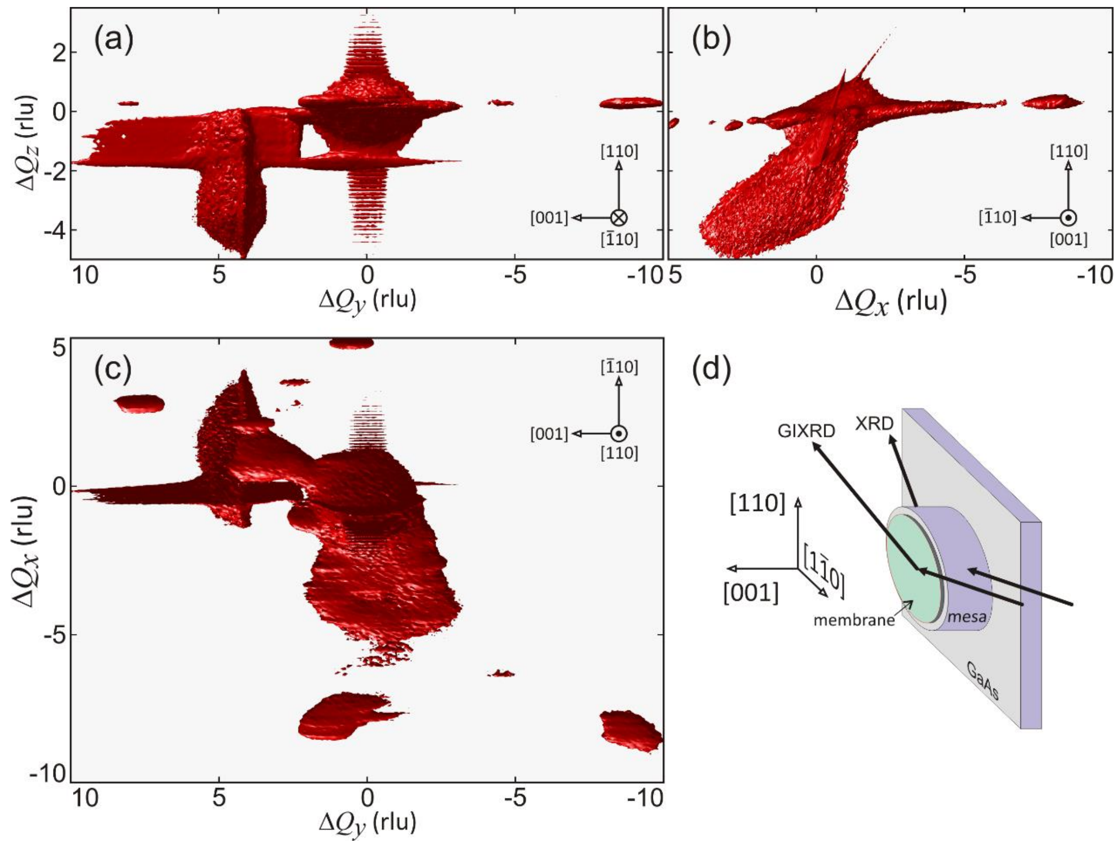

Supp. Fig. 3: Three-dimensional Reciprocal space map of a 10 nm $In_{0.4}Ga_{0.6}As$ layer deposited on the membrane showing iso-intensity surfaces. (a-c) View from different perspectives regarding the crystal frame in (d). GIXRD from membranes is seen at ΔQ_y > 4 rlu. 1rlu = 0.01Å^{-1}.

Room temperature photoluminescence data

We provide additional photoluminescence (PL) data obtained at room temperature (RT) using a macro PL setup. The samples are excited with a wavelength of 432 nm at a power of ca. 12 mW using a ca. 0.1 mm spot size – this covers roughly one entire mesa. Samples are not optimised for RT and we expect therefore a weak and rather broad signal. The obtained PL spectrum is depicted in Suppl. Fig. 4.

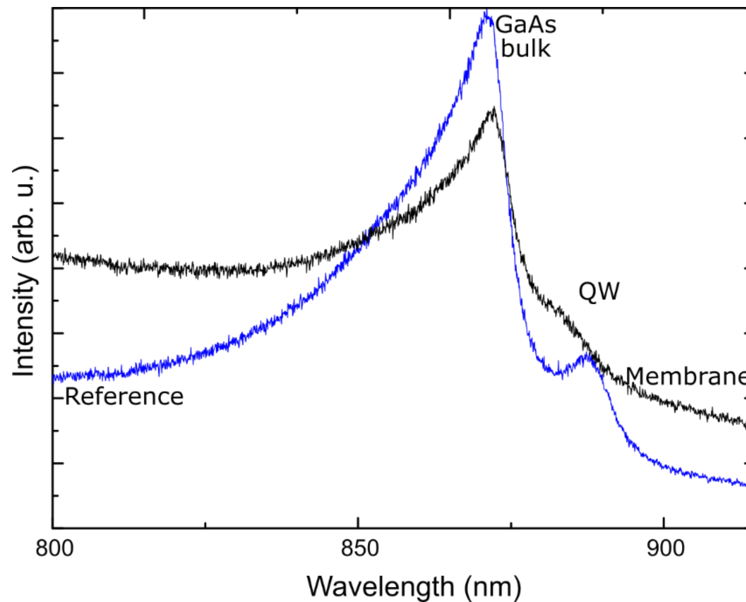

Supp. Fig. 4: RT PL data obtained from the reference quantum well grown on the bulk GaAs (001) substrate (blue curve) and the quantum well grown on the released and wrinkled membrane (black curve).

Analyzing the PL data, we observe that the spectra are dominated by the GaAs bulk band gap emission with peak at ca. 870 nm. Furthermore, we can identify a weak quantum well emission at 888 nm and 884 nm for the reference and the membrane-based sample, respectively. As the quantum well has only 10 nm InAlGaAs barriers, its confinement is expected to be rather weak at RT. As we use a larger spot size, we notice the already discussed inhomogeneity of the quantum well grown on the wrinkled membrane giving rise to the large and not pronounced peak. Finally, we observe for both samples a tail of the PL up to 780 nm (not fully shown in the spectrum), which we ascribe to the emission of the InAlGaAs barrier. A broader emission of InAlGaAs is also observed for membrane due to the winkles.

Considering that structures are not optimized yet, the observation of RT PL for the membrane sample is a good indication that membrane-based structures are suitable for device growth working at ambient conditions.

Transfer of a 15-nm GaAs membrane to a new host substrate

To demonstrate our ability to transfer thin semiconductor membranes to a new host substrate prior overgrowth, we documented a transfer of a 15-nm thick GaAs membrane. An initial heterostructure was grown by molecular beam epitaxy on top of a GaAs (001) wafer consisting of a 100-nm GaAs buffer, a 300-nm thick $Al_{0.9}Ga_{0.1}As$ layer and a top 15-nm GaAs layer. A transfer of the top GaAs layer to a new host substrate (Si with photo resist) is documented in Suppl. Fig. 5.

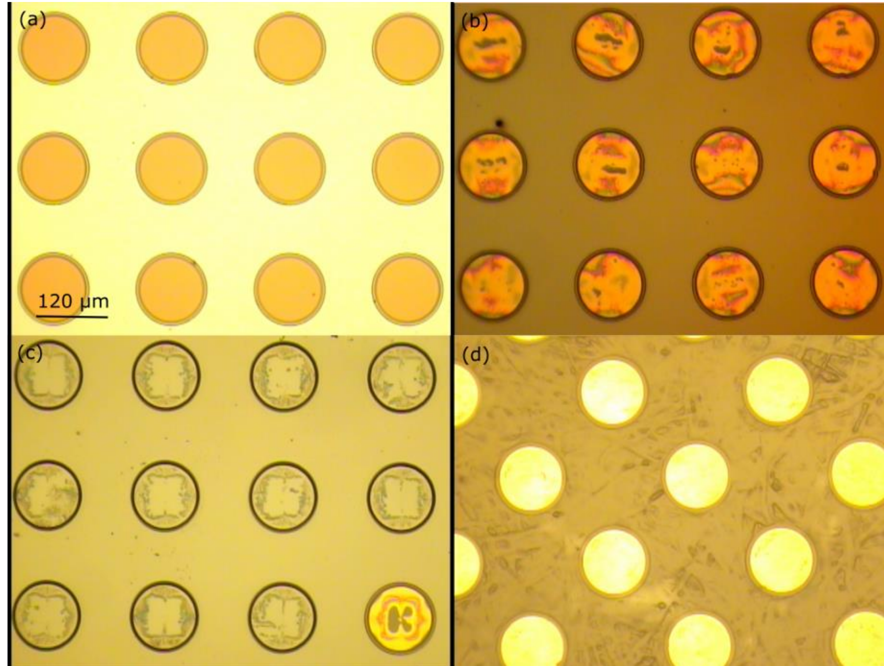

Supp. Fig. 5: Light microscopy images documenting the transfer of a 15-nm membrane. (a) Defined mesas with ca. 100 µm diameter. The resist is still on top of the unreleased GaAs top layer and a slight lateral under etching is visible. (b) Released membranes on top of the mesa structure. (c) Substrate without the membranes. In the lower right corner one membrane was not transferred, most likely due to an incomplete release. (d) Transferred membranes on top of a photo resist coated host substrates. The photoresist covering the now bottom of the transferred membrane is observable. Even so, transfer was done by simply pressing the release structure to the host substrate and then removing the initial substrate, the alignment and order of the initial lithographical defined mesa is preserved.

Suppl. Fig. 5(a) depicts a light microscopy image of the sample with an initial mesa structure defined. For the process, the sample was covered with photo resist and UV photolithography carried out to define the pattern. This was followed by a etching step using a H_3PO_4:H_2O_2:H_2O (1:2.5:10) solution. The photo resist is sill on top of the mesas and a slight lateral under etching - common for this kind of process - is observable. The top 15-nm GaAs layer was released in a successive selective etching step using HF (3 vol%) and a light microscopy image of the obtained structure is seen in Suppl. Fig. 5(b). It is important to carry out the next step quickly after release as with time the membranes start to stick to the substrate. For transfer, the host substrate was coated with photoresist and the initial substrate is pressed upside down into the resist. The resist acts as adhesion layers and the released membranes stick to the new substrate.[1] In Suppl. Fig. 5(c), a light microscopy image of the substrate after transfer is seen. Compared with Suppl. Fig. 5(a) and (b), the image demonstrates that the membranes were removed from the initial substrate –

for demonstration propose, we chose one of the few spots were transfer did not work and a membrane is still on the substrate in the lower right corner illustrating the difference between transferred and not transferred substrate areas. Finally, the membranes on top of the new host substrate are seen in Suppl. Fig. 5(d). Careful inspection of the light microscopy image reveals the initial top photo resist that's now the bottom of the membrane and doing the adhesion to the new substrate. The high quality of the membrane was later demonstrate as the sample was used for a advanced x-ray diffraction study.[2] More advanced transfer processes, e.g. using soft imprint lithography,[3] result in cleaner samples that would be suited for overgrowth.

References

(1) Rastelli, A.; Ding, F.; Plumhof, J. D.; Kumar, S.; Trotta, R.; Deneke, C.; Malachias, A.; Atkinson, P.; Zallo, E.; Zander, T.; et al. Controlling Quantum Dot Emission by Integration of Semiconductor Nanomembranes onto Piezoelectric Actuators. *Phys. Status Solidi B-Basic Solid State Phys.* **2012**, *249* (4), 687–696. https://doi.org/10.1002/pssb.201100775.

(2) Freitas, R. O.; Deneke, C. F.; Malachias, Â.; Darin, G.; Morelhão, S. L. Measuring Friedel Pairs in Nanomembranes of GaAs (001). *J. Nanoparticle Res.* **2013**, *15* (4), 1–7. https://doi.org/10.1007/s11051-013-1527-3.

(3) Rogers, J. A. ELECTRONICS A Diverse Printed Future. *Nature* **2010**, *468* (7321), 177–178.